

# THE 4TH INTERNATIONAL CONFERENCE ON ALUMINUM ALLOYS

## RATE-CONTROLLING PROCESSES FOR CREEP CRACK GROWTH IN Al-Li ALLOYS

S.P. Lynch and R.T. Byrnes

Aeronautical and Maritime Research Laboratory, Defence Science and Technology Organisation,  
Department of Defence, Fishermens Bend, Victoria 3207 AUSTRALIA

### Abstract

Creep crack growth rates in a vacuum-refined 8090 Al-Li-Cu-Mg alloy extrusion, with very low alkali metal impurity contents (<1ppm) and low hydrogen levels, have been determined as a function of stress-intensity factor and temperature for the S-L crack-plane orientation. These data have been compared with previous data for S-L creep crack growth in 8090 plate with normal commercial levels of alkali metals (3-10ppm) and hydrogen. The similar crack growth rates and activation energies for cracking for the plate and extrusion suggest that previous indications that impurities might be responsible for the poor creep cracking resistance of Al-Li alloys (compared with conventional Al alloys) can be discounted. The rates of development of low-temperature (-196°C) intergranular embrittlement as a function of ageing temperature for re-solution treated and quenched 8090 plate have also been studied. The activation energies of the processes producing embrittlement were ~0.83eV for ageing temperatures between 0 and 60°C, and ~0.44eV between 60 and 150°C. These values and changes in activation energy are similar to those observed for creep cracking in the 8090 plate. These and other observations suggest that creep crack growth is caused by lithium diffusion to and segregation at grain boundaries, with segregation during creep cracking being promoted by the presence of hydrostatic stresses or localised strains around crack tips.

### Introduction

Al-Li alloys with densities ~10% lower than other Al alloys have been developed to the stage where many of their properties are as good as, or better than, conventional 2xxx and 7xxx series alloys. The resistance of Al-Li alloys to creep crack growth, however, is often much lower than that of conventional 2xxx and 7xxx alloys [1-4]. Creep cracking occurs along grain boundaries, and takes place readily in both 8090 and 2090 Al-Li alloys for product forms where there are continuous, relatively planar, intergranular crack paths normal to the applied stress, e.g. S-L crack-plane orientations for unrecrystallised plate, S-L and T-L orientations for extrusions, and all orientations for recrystallised sheet. In these cases, cracking has been observed at appreciable rates at stress-intensity factors as low as 10% of  $K_{Ic}$  or  $K_{Ic}$  at temperatures as low as 60°C [1,2].

It was suggested [1,2] that the presence of liquid alkali-metal phases and segregation of lithium at grain boundaries were probably responsible for the poor creep cracking resistance of Al-Li alloys. However, the relative importance of alkali-metal impurities and lithium segregation was not established. It was also not clear what processes controlled the rate of crack growth. Arrhenius plots of the rate of creep cracking in 8090-T8771 plate (at high K) versus the inverse of the absolute temperature showed that there was a distinct change in slope at  $\sim 120^{\circ}\text{C}$ , with activation energies for cracking  $\sim 0.89\text{eV}$  between 50 to  $120^{\circ}\text{C}$  and  $\sim 0.58\text{eV}$  between 120 and  $200^{\circ}\text{C}$  [1].

Observations in the present work of (i) creep cracking in Al-Li alloys with very low concentrations of alkali-metal impurities, and (ii) the incidence of intergranular fracture (at  $-196^{\circ}\text{C}$ ) as a function of ageing time and temperature, suggest that lithium diffusion to, and segregation at, grain boundaries controls the kinetics of creep cracking, and that alkali-metal impurities play only a minor role.

### Experimental Procedure

An 8090 plate and an extrusion with a similar composition (Table I) were tested. The 45 mm thick plate was the same as that used in a previous study of creep crack growth and contains alkali-metal and hydrogen levels typical of most commercially produced material. The extrusion (13 x 45 mm cross-section) was produced from experimental material melted and cast under vacuum to reduce alkali-metal and hydrogen levels to low levels [5]. The extrusions were solution-treated, quenched and aged to near peak-hardness (48 h at  $150^{\circ}\text{C}$ ). Bolt-loaded double-cantilever beam (DCB) specimens were machined from the extrusion and tested in the short-transverse (S-L) orientation at  $60\text{-}180^{\circ}\text{C}$  in dry air, as described in previous work on creep crack growth [1].

Table I. Composition of the 8090 plate (at mid-thickness) and the extrusion

	Amount (wt %)						Amount (wt.ppm) <sup>+</sup>		
	Li	Cu	Mg	Zr	Fe	Si	Na	K	H
Plate:	2.30	1.03	0.62	0.12	0.04	0.03	2.5	2	0.7
Extrusion:	2.40	1.26	0.56	0.07			0.45	0.1	0.15

<sup>+</sup> Alkali-metal impurities were determined by atomic-absorption spectroscopy, neutron-activation analysis, or glow-discharge mass-spectroscopy. Hydrogen was measured by a nitrogen-carrier fusion technique (LECO Hydrogen Analyser).

Studies of fracture as a function of ageing time and temperature in the 8090 plate involved: (i) machining specimens (25 x 7 x 5 mm) with a notch at one edge so that fracture would occur in the S-L crack plane at the mid-thickness position, (ii) re-solution treating specimens at  $545^{\circ}\text{C}$ , quenching into water at  $\sim 0^{\circ}\text{C}$ , and ageing at  $3.5$  to  $150^{\circ}\text{C}$  for various times, and (iii) immersing specimens (clamped in a holder) in liquid nitrogen for  $>20$  minutes and then rapidly fracturing specimens by bending in air before appreciable increases in temperature occurred.

## Results

### Creep Crack Growth

Rates of creep crack growth at high stress-intensity factors ( $K$ ) at  $120^\circ\text{C}$  for the extrusion were  $\sim 1\text{mm/h}$ , and threshold  $K$  values were  $\sim 5\text{MPa}\sqrt{\text{m}}$  (Fig. 1), as observed for 8090 T8771 plate in previous work [1]. An Arrhenius plot of creep crack velocity versus the inverse of temperature for the extrusion was also similar to that in the 8090 plate — both exhibiting a change in slope at  $\sim 120^\circ\text{C}$ , with activation energies for cracking  $\sim 0.89\text{eV}$  between  $60$  and  $120^\circ\text{C}$  and  $\sim 0.6\text{eV}$  between  $120$  and  $200^\circ\text{C}$  (Fig. 2). Fracture surfaces produced by both overload and creep crack growth exhibited dimpled and relatively featureless intergranular areas (Fig. 3). Dimples were more common, and were more elongated (normal to the direction of crack growth) for creep fractures than for overload fractures.

### Fracture at $-196^\circ\text{C}$

8090 plate specimens tested at  $-196^\circ\text{C}$  after re-solution treating and quenching exhibited ductile, transgranular fracture surfaces. Increasing proportions of featureless intergranular fracture were observed after ageing for progressively longer times at a given temperature and after ageing at higher temperatures for a given time (Fig. 4). Arrhenius plots of the times to produce 50% intergranular fracture versus the inverse of absolute temperature had slopes corresponding to activation energies for embrittlement of  $\sim 0.83\text{eV}$  between  $3.5$  and  $60^\circ\text{C}$  and  $\sim 0.44\text{eV}$  between  $60$  and  $150^\circ\text{C}$  (Fig. 5).

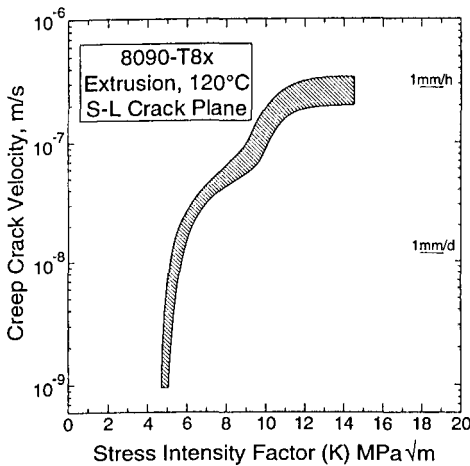


Figure 1. Plot of creep crack velocity at  $120^\circ\text{C}$  vs. stress-intensity factor for the low-impurity 8090 extrusion.

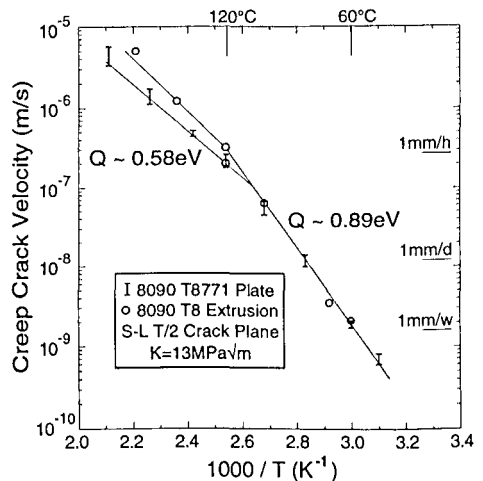


Figure 2. Arrhenius plots of creep crack velocity at high  $K$  vs. inverse absolute temperature for the low-impurity 8090 extrusion (present work), and the 8090 plate (previous work [1]).

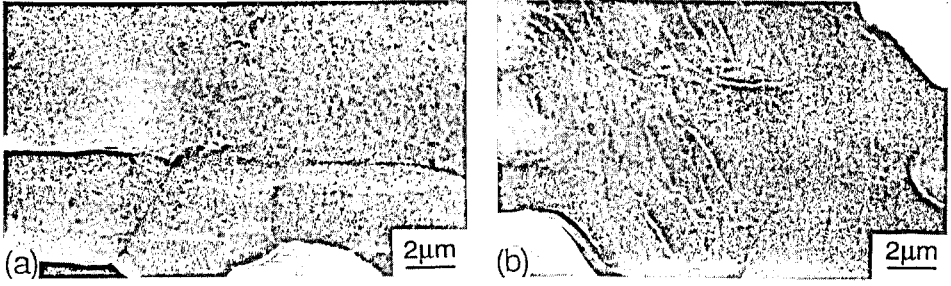


Figure 3. SEM of fracture surfaces produced by (a) overload at 20°C, and (b) creep crack growth at 180°C, for the extrusion.

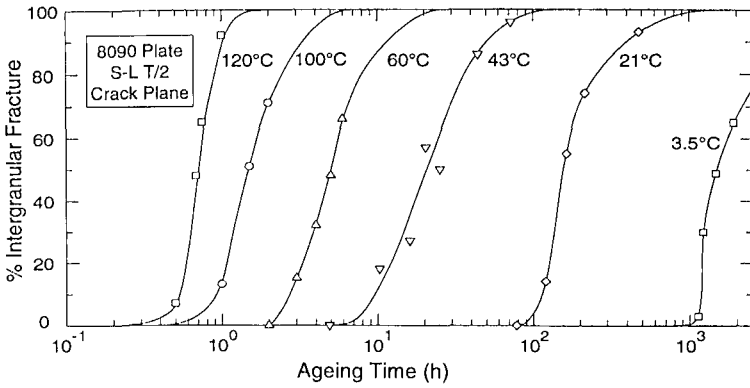


Figure 4. Effect of ageing time and temperature on the extent of intergranular fracture at -196°C for re-resolution treated and quenched 8090 plate.

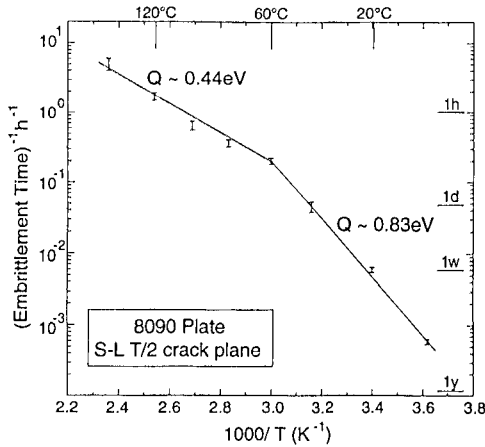


Figure 5. Arrhenius plots of the times to produce 50% intergranular fracture vs. inverse absolute temperature in 8090 plate derived from the data in figure 4.

## Discussion

Intergranular fracture at  $-196^{\circ}\text{C}$  in very underaged material is most probably associated with lithium diffusion to, and segregation at, grain boundaries since:

- (i) analytical TEM indicates that lithium segregation develops at ageing times corresponding to the occurrence of intergranular fracture [6],
- (ii) matrix and grain-boundary precipitation do not develop to any significant extent for these ageing times and temperatures [6],
- (iii) there is no evidence of impurity segregation [7], and alkali-metal phases would be solid at  $-196^{\circ}\text{C}$  and therefore not embrittling, and
- (iv) the activation energy for embrittlement (at the lower temperatures) is close to that for lithium diffusion to grain boundaries determined from the kinetics of precipitate-free-zone (PFZ) growth [6,8].

Since the activation energies for creep cracking (for both the plate and extrusion) are fairly similar to those for embrittlement of very under-aged material tested at  $-196^{\circ}\text{C}$ , with both exhibiting a decrease at higher temperatures, the rate of creep cracking is probably also controlled by lithium diffusion to, and segregation at, grain boundaries. Different processes can sometimes have similar activation energies so that one cannot generally reach such a conclusion with any confidence. However, the fact that the activation energies for both creep cracking and low-temperature embrittlement decrease at higher temperatures in the present case does strongly suggest that the rate-controlling processes are the same.

The change in slope of Arrhenius plots indicates that two consecutive processes with different activation energies are involved. Lithium diffusion to grain boundaries is probably the rate-controlling process at the lower temperatures, while incorporation (or re-arrangement) of lithium atoms in the grain-boundary structure, perhaps to form a two-dimensional phase, could be the rate-controlling process at the higher temperatures. Studies by the present authors [6,9] showing that the texture (which determines the grain-boundary-misorientation distribution) influences the kinetics of embrittlement supports this suggestion.

Thermodynamic considerations suggest that aluminium should be embrittled by segregation of lithium [10]. Presumably weakening of interatomic bonds across grain boundaries is involved, but the precise mechanism has not been established. The presence of elongated dimples on fracture surfaces (in some areas) indicates that fracture involves the coalescence of crack tips with elongated voids ahead of cracks. Featureless intergranular areas may be produced either by a similar process on a scale not producing resolvable dimples or by a 'decohesion' process. Segregation of hydrogen as well as lithium, perhaps forming a two-dimensional film of lithium hydride [11], cannot be ruled out, but the similar crack growth kinetics for material with high (0.7 ppm) and low (0.15 ppm) hydrogen contents suggest that hydrogen segregation is not a critical factor.

Alkali-metal impurities, which result in discrete low melting point phases along grain boundaries, do not appear to play a major role in promoting creep crack growth since the extrusion with  $<1\text{ppm}$  impurities behaved the same as the plate with  $\sim 5\text{ppm}$  impurities. The presence of alkali-metal phases can, however, result in the formation of distinctive features on fracture surfaces.

Cleavage-like and brittle intergranular islands, centred on inclusions (with which liquid alkali-rich phases are associated), surrounded by more ductile areas are often observed [1,2]. The 'brittle' cracks associated with the embrittling liquid phase extend only a short distance before the (limited) supply of liquid metal is exhausted. The creep-cracking resistance is therefore controlled by fracture of material between the liquid-metal induced cracks. For alloys with high alkali metal contents (~40 ppm), liquid-metal-induced brittle cracking is quite extensive and rates of creep crack growth are somewhat higher than in alloys with low ( $\leq 10$  ppm) alkali-metal contents [1].

Lithium segregation at grain boundaries is probably present to a significant extent after ageing to T8 conditions (contributing to a low resistance to rapid overload fracture [6,12,13]), with increases in segregation occurring when material is stressed at elevated temperature resulting in creep crack growth. Evidence that lithium segregation facilitates (S-L) overload fracture has been discussed in detail in previous papers [6,12,13] and is based especially on the effects of re-ageing treatments. For example, re-ageing for short times (~5 mins) at 200°C after first ageing for 32 h at 170°C results in a fracture toughness almost double that of the single-aged condition, with only a small decrease in strength and no significant change in microstructure. It was proposed that re-ageing for short times at higher second ageing temperatures increased toughness by decreasing the extent of lithium segregation at grain boundaries — the segregated lithium rapidly diffusing to and being incorporated into grain-boundary precipitates before an increased flux of lithium from the matrix reached the grain boundary. Subsequent ageing of double-aged material at 60 - 160°C resulted in re-embrittlement with an activation energy ~0.93eV, i.e. close to that observed for (i) PFZ width growth and (ii) embrittlement at -196°C for very underaged material, suggesting that diffusion of lithium to grain boundaries and re-segregation of lithium were responsible for re-embrittlement.

The creep-crack-growth rates of double-aged material (tested at the same initial K value as single-aged material) were **initially** much lower than single-aged material — with little crack growth occurring in double-aged material until exposure times approached re-embrittlement times [2]. Subsequent creep crack growth then occurred at similar rates as in single-aged material. These observations further support the conclusion that lithium segregation at grain boundaries is responsible for creep crack growth.

Exposure of **unstressed** T8 aged specimens at elevated temperatures for times corresponding to those used for creep-crack-growth testing produced little, if any, decrease in toughness, even though some lithium diffusion to grain boundaries would have occurred. Thus, it appears that the stress (or plasticity) either increases diffusion rates or increases the level of segregation. Lithium reaching grain boundaries by lattice diffusion will not only segregate at grain boundaries but will also diffuse along grain boundaries to precipitates which act as sinks for lithium. If such sinks were not effective, as would be the case in the plastic zone ahead of cracks if precipitate-matrix interfaces had decohered, then lithium segregation may reach higher levels than that in the absence of plasticity. Alternatively, an effect of stress **per se**, rather than the deformation it produces, could cause an increase in diffusion rates to boundaries or an increase in the amount of segregation (Fig. 6).

Stress-enhanced segregation of impurity or alloying elements has been proposed previously to account for the phenomenon of intergranular creep crack growth in other materials [14-16]. It

has been suggested that high hydrostatic stresses just ahead of cracks result in dilatation of the lattice thereby promoting diffusion of embrittling atoms to boundaries near crack tips; dilatation of the grain-boundary structure itself could also result in increased levels of segregation. Experimental evidence for stress-enhanced segregation has been obtained for the steel-sulphur system, although there is some disagreement regarding the exact diffusion paths by which sulphur impurities reach grain boundaries near or at crack tips [14,15]. Stress-enhanced segregation to grain boundaries has also been proposed to account for intergranular creep crack growth in Cu-8% Sn alloys [16] — a more analogous system to Al-Li than the steel-sulphur system since both tin and lithium are present as major alloying elements (8 - 10at.%) where the solute atoms are larger than the solvent atoms.

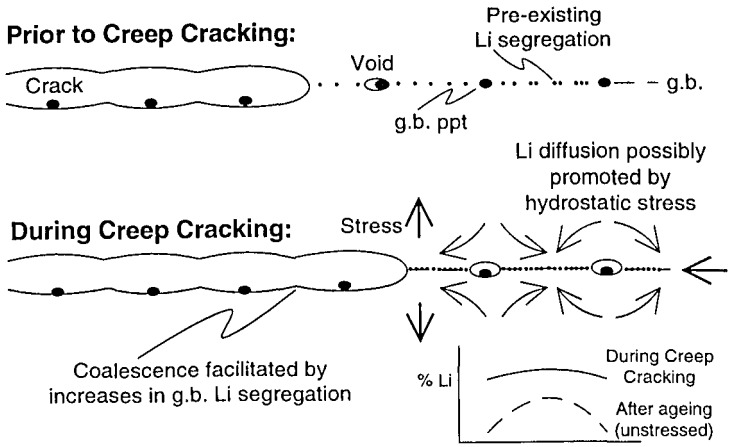


Figure 6. Schematic diagram illustrating possible mechanism of creep crack growth.

Conclusions

1. Alkali-metal and hydrogen impurities appear to play little or no role during creep cracking since the creep-crack-growth resistance of an Al-Li-Cu-Mg alloy extrusion with low alkali-metal impurities (< 1 ppm) and low hydrogen levels (< 0.2 ppm) was similar to that of an 8090 plate with ~5 ppm alkali impurities and ~0.7 ppm hydrogen. Crack velocities at 120°C were ~1 mm/h at high K values and threshold K values were ~5 MPa  $\sqrt{m}$  — a much lower creep-cracking resistance than that of non-lithium containing Al alloys.
2. Comparisons of the kinetics of creep cracking with the kinetics of embrittlement of re-solution-treated and quenched material tested at -196°C after ageing for different times and temperatures, and other observations, strongly suggest that lithium diffusion to grain boundaries controls the rate of creep cracking below 120°C. At higher temperatures, incorporation of lithium atoms into the grain-boundary structure may possibly be the rate-controlling process.
3. Creep cracking in Al-Li alloys may be an example of a more general phenomenon, namely, stress-induced segregation and embrittlement — other examples being the steel-sulphur system and the copper-tin system.

### Acknowledgements

The Al-Li-Cu-Mg extrusion with low impurity levels was kindly supplied by Comalco Research Centre, Melbourne, Australia.

### References

1. S.P. Lynch, Mater. Sci. and Engng. A 136 (1991), 45.
2. S.P. Lynch, Mater. Sci. and Tech. 8 (1992), 34.
3. K. Sadananda and K.V. Jata, Metall. Trans. A, 19 (1988), 847.
4. N. Benhood, H. Cai, J.T. Evans, and N.J.H. Holroyd, Mater. Sci. and Engng. A119 (1989), 23.
5. D Webster, U.S. Patent No. 5,085,830, 1992
6. S.P. Lynch, A.R. Wilson, and R.T. Byrnes, Mater. Sci. and Engng. A172 (1993), 79.
7. W.S. Miller, M.P. Thomas, D.J. Lloyd and D. Creber, Aluminium-Lithium Alloys III, ed. C. Baker, P.J. Gregson, S.J. Harris and C.J. Peel (Institute of Metals, London, 1986), 584.
8. W.S. Miller, J. White and M.A. Reynolds, Proc. 1st Int. SAMPE Metals Conf., Vol. 1 (1987), 308.
9. S.P. Lynch and R.T. Byrnes, unpublished work, 1993.
10. M.P. Seah, Acta Metall. 28 (1990), 955.
11. J.J Lewandowski and N.J.H. Holroyd, Mater. Sci. and Engng. A123 (1990), 219.
12. S.P. Lynch, Mater. Sci. and Engng. A 136 (1991), 25.
13. S.P. Lynch, R. Byrnes, R.B. Nethercott, A. Bragianos, and A. Crosky, Aluminium-Lithium, ed. M. Peters and P.-J. Winkler, (DGM Informationsgesellschaft mbH, Oberursel, Germany, 1992), Vol. 1, 391.
14. C.A. Hipsley, Acta Metall. 35 (1987), 2399.
15. J.J. Lewandowski, C.A. Hipsley, M.B.D. Ellis, and J.F. Knott, Acta Metall. 35 (1987), 593.
16. E.V. Barrera, M. Menyhard, D. Bika, B. Rothman, and C.J. McMahon, Jr., Scripta Metall. 27 (1992), 205.